Rotational quenching of CO due to H_2 collisions

Benhui Yang and P. C. Stancil

Department of Physics and Astronomy and the Center for Simulational Physics,

The University of Georgia, Athens, GA 30602-2451

yang@physast.uga.edu, stancil@physast.uga.edu

N. Balakrishnan

Department of Chemistry, The University of Nevada Las Vegas, Las Vegas, NV 89154

naduvala@unlv.nevada.edu

R. C. Forrey

Department of Physics, Penn State University, Berks Campus, Reading, PA 19610

rcf6@psu.edu

Received _____; accepted _____

ABSTRACT

Rate coefficients for state-to-state rotational transitions in CO induced by both para- and ortho-H_2 collisions are presented. The results were obtained using the close-coupling method and the coupled-states approximation, with the CO-H_2 interaction potential of Jankowski & Szalewicz (2005). Rate coefficients are presented for temperatures between 1 and 3000 K, and for CO($v = 0, j$) quenching from $j = 1 - 40$ to all lower j' levels. Comparisons with previous calculations using an earlier potential show some discrepancies, especially at low temperatures and for rotational transitions involving large $|\Delta j|$. The differences in the well depths of the van der Waals interactions and the anisotropy of the two potential surfaces lead to different resonance structures in the energy dependence of the cross sections which influence the low temperature rate coefficients. Applications to far infrared observations of astrophysical environments are briefly discussed.

Subject headings: molecular processes —- molecular data — ISM: molecules

1. INTRODUCTION

Molecular hydrogen and carbon monoxide are the most abundant molecular species in the majority of interstellar environments, and they play important roles in determining the physics and chemistry of diffuse clouds (Herbst 2001). CO is observed in diffuse clouds in absorption in the ultraviolet (UV) and visible and in emission at infrared (IR) wavelengths (Snow & McCall 2006), revealing the physical and chemical complexity along these lines of sight. As an example, Liszt (2006, 2007) recently investigated the formation, fractionation, and rotational excitation of CO in H_2 bearing diffuse H I clouds. Due to its small rotational constant, CO can be easily rotationally excited by collisions with other species in interstellar gas, mostly H_2, with CO rotational lines providing important diagnostics of gas density and temperature. The abundance ratio, CO/H_2, is assumed to be roughly constant in dense molecular gas, as such, CO is often used as a tracer of H_2, as the latter is difficult to detect in emission in cold environments. The observed CO abundance is therefore used to estimate the total H_2 content (Sonnentrucker et al. 2007).

In environments with an intense UV field, the radiation can drive the chemistry and internal level populations out of equilibrium. In such situations, a photodissociation region (PDR) resides at the interface of the hot H II region and the cold molecular region. In recent years various codes which model the physics and chemistry of PDRs have been developed with an emphasis on the excitation mechanisms of both H_2 and CO (van Dishoeck & Black 1988; Warin et al. 1996; Le Petit et al. 2006; Shaw et al. 2005; Röllig et al. 2007).

In more dense environments such as low-mass dwarf stars (i.e., M, L, or T dwarfs), CO is an important opacity source and its infrared line list can be obtained quite accurately (Pavlenko & Jones 2002; Jones et al. 2005). It has also been observed in the dayside spectrum of the transiting hot-Jupiter extrasolar giant planet (EGP) HD 189733b (Swain et al. 2009). While molecular level populations are typically treated in local

thermodynamic equilibrium (LTE) in stellar and planetary atmospheres, Schweitzer et al. (2000) have pointed out that non-LTE conditions may exist in very cool stellar atmospheres or in cases where the temperature of the incident radiation, i.e. close-in EGPs, is much different from the kinetic temperature of the gas.

Due to the astrophysical importance of molecular hydrogen and carbon monoxide, the CO-H_2 collisional system has been the subject of numerous experimental (Kudian et al. 1967; Butz et al. 1971; Kupperman et al. 1973; Bouanich & Brodbeck 1973; Nerf & Sonnenberg 1975; Brechignac et al. 1980; Andresen et al. 1982; Picard-Bersellini et al. 1983; Schramm et al. 1991; Drascher et al. 1998; McKellar 1990, 1991, 1998; Antonova et al. 2000) and theoretical (Green & Thaddeus 1976; Prisette et al. 1978; Flower et al. 1979; Poulsen 1982; Schinke et al. 1984; Bacic et al. 1985a,b; Jankowski & Szalewicz 1998, 2005; van Hemert 1983; Parish et al. 1992; Danby et al. 1993; Salazar et al. 1995; Reid et al. 1997; Mengel et al. 2001; Baker & Flower 1984; Flower & Launay 1985; Flower 2001; Antonova et al. 2000; Wernli et al. 2006; Yang et al. 2006a,b) studies. Quantitative determinations of state-to-state cross sections and rate coefficients for CO-H_2 collisions are crucial to numerical models of various astrophysical environments, such as those highlighted above. However, as measurements of these quantities are difficult, numerical models often rely on cross sections and rate coefficients derived from theoretical methods. In a highly-cited work, Green & Thaddeus (1976) performed close-coupling calculations of rate coefficients based on an approximate CO-H_2 potential surface. Since then, a number of quantum scattering calculations were carried out on various potential energy surfaces (PESs). In this work, we have performed comprehensive calculations of state-to-state cross sections in an effort to develop a complete database of rotational quenching rate coefficients, but utilizing a more recent, and presumably more accurate PES. In the following sections, the choice of the potential surface, the adopted scattering approach, and the results are discussed. We briefly highlight important astrophysical applications of the current CO-H_2

rate coefficients for modeling of far IR (FIR) observations.

2. THE POTENTIAL ENERGY SURFACE

A number of PESs (Prisette et al. 1978; Flower et al. 1979; Poulsen 1982; Schinke et al. 1984; Bacic et al. 1985a; Jankowski & Szalewicz 1998, 2005) have been developed for the CO-H_2 complex. One of the most accurate surfaces was given by Jankowski & Szalewicz (1998) who calculated a four-dimensional, rigid-rotor PES referred to as V_{98}. This surface was constructed using the symmetry-adapted perturbation theory (SAPT) method with high-level electron correlation effects. An analytical fit of the *ab initio* PES has a global minimum of 109.3 cm^{-1} at the intermolecular separation of 7.76 a_0 for the linear geometry with the C atom pointing toward H_2. Antonova et al. (2000) adopted V_{98} in their calculations of state-to-state cross sections for CO rotational excitation at collision energies between 795 and 991 cm^{-1} which were found to be in good agreement with their measurements. The V_{98} PES was also utilized in second virial coefficient calculations for mixtures of hydrogen and CO (Gottfried & McBane 2000). A comparison with experimental data suggested that the van der Waals well of the V_{98} PES is too deep by 4%-9%, though it represents an improvement over earlier surfaces. The V_{98} surface has also been used in full coupled-channel cross section and rate coefficient calculations for rotationally inelastic scattering of CO by para- and ortho-H_2 (Flower 2001; Mengel et al. 2001). However, because the attractive well of V_{98} was presumed to be too deep, Mengel et al. (2001) modified the PES by merely multiplying the surface by a constant factor of 0.93 which was subsequently used in their scattering calculations.

A newer CO-H_2 PES was reported by Jankowski & Szalewicz (2005), referred to as V_{04}. To improve the surface accuracy, they adopted the coupled-cluster method with single, double, and noniterative triple excitations [CCSD(T)] and the supermolecular approach.

The V_{04} surface was obtained on a five-dimensional grid including the dependence on the H-H separation, but with the CO molecule taken to be rigid with the C-O separation set to the value of the C-O distance averaged over the CO ground state vibrational wave function. The PES was then obtained by averaging over the intramolecular vibration of H_2 to yield a four-dimensional rigid-rotor surface. Similar to V_{98}, an analytical fit of the V_{04} was presented which has a global minimum of 93.05 cm^{-1}, or 16.22 cm^{-1} shallower than V_{98}. Jankowski & Szalewicz (2005) used V_{04} to calculate the rovibrational energy levels for the para- and ortho-H_2-CO complex as well as the second virial coefficient. The rovibrational energies were found to agree with the experimental values of McKellar (1998) for para-H_2 to within 0.1 cm^{-1} while a scaling of V_{04}, resulting in a deepening of the well depth by 4 cm^{-1}, was needed to match the measured second virial coefficients. V_{04} may be too shallow though it is possible that the experimental second virial coefficients are systematically too low (Jankowski & Szalewicz 2005). Comparative studies of collisional cross sections using the two surfaces have been presented in our earlier work (Yang et al. 2006a) and by Wernli et al. (2006). In Yang et al. (2006a), calculations with the V_{04} surface gave cross sections in excellent agreement with the state-to-state measurements of Antonova et al. (2000).

3. THEORETICAL APPROACH

The theory for the scattering of two linear rigid rotors has been developed in Green (1975) and Heil et al. (1978). The calculations presented here were performed for collision energies between 10^{-5} and 10,000 cm^{-1} by applying both the close-coupling (CC) method and the coupled-states (CS) approximation. All the CC and CS calculations were performed using the nonreactive scattering code MOLSCAT (Hutson & Green 1994). In the quantum scattering calculations, the coupled-channel equations were integrated using the modified

log-derivative Airy propagator of Alexander & Manolopoulos (1986) with a variable step size. The largest Legendre terms adopted in the potential expansion for H_2 and CO were, respectively, 8 and 10. The numbers of Gauss integration points used in projecting angular components of the potential were 10, 11, and 12 for integration in θ_1, θ_2, and ϕ, respectively. The propagation was carried out to a maximum intermolecular separation of $R = 100$ Å. At each energy, a sufficient number of total angular momentum partial waves was included to ensure convergence of the state-to-state cross sections to within 1%. The maximum value of the total angular momentum quantum number J employed in the calculations was 300. Since, the computation time for CC calculations scales as $j_{\rm max}^6$, the CS method is adopted for energies greater than 800 $\rm cm^{-1}$ which results in considerable time savings with a scaling proportional to $j_{\rm max}^4$, where $j_{\rm max}$ is the maximum size of the rotational basis. Further details about the scattering calculations can be found in Yang et al. (2006a,b). The adopted rotational constants for H_2 and CO are 60.853 $\rm cm^{-1}$ (Huber & Herzberg 1979) and 1.9225 $\rm cm^{-1}$ (Lovas et al. 1979), respectively. Hereafter, j_1 denotes the rotational quantum number for H_2, and likewise j_2 for CO. In the present study, we adopted the four-dimensional PES for the CO-H_2 complex, V_{04}, of Jankowski & Szalewicz (2005).

Calculations of the collision energy dependence of state-to-state quenching cross sections for initial rotational states of CO, j_2=1, 2, $\cdots$, 40, by collisions with both para- and ortho-H_2 (i.e., $j_1 = 0, 1$, respectively) were performed. The cross sections were thermally averaged over the kinetic energy distribution to yield state-to-state rate coefficients from specific initial rotational states j_2 as functions of the temperature T,

$$k_{j_2 \to j_2'}(T) = \left(\frac{8}{\pi\mu\beta}\right)^{1/2} \beta^2 \int_0^\infty E_k \sigma_{j_2 \to j_2'}(E_k) \exp(-\beta E_k) dE_k \qquad (1)$$

where $\sigma_{j_2 \to j_2'}$ is the rotational transition cross section with j_2 and j_2' being respectively the initial and final rotational quantum number of CO, μ is the reduced mass of the CO-H_2

complex, E_k the kinetic energy, and $\beta = (k_B T)^{-1}$, where k_B is the Boltzmann constant.

4. RESULTS AND DISCUSSION

All state-to-state cross sections and rate coefficients for quenching are available on the UGA Molecular Opacity Project website (www.physast.uga.edu/ugamop/). The rate coefficients are also available in the format of the Leiden Atomic and Molecular Database (LAMDA, Schöier et al. 2005) on our website and the LAMDA site (www.strw.leidenuniv.nl/∼moldata/). Fig. 1 shows typical examples of state-to-state cross sections for $j_2 = 5$ and 20 for collisions with para-H_2. A number of resonances are evident between 10^{-2} and 10^2 cm^{-1} which result in significant modulation in the rate coefficients. However, the magnitude of the resonances are seen to decrease with j_2. Cross sections for some other j_2 can be found in Yang et al. (2006a,b). The agreement between the CC and CS calculations is shown to be excellent with a difference typically better than ∼20%, justifying the adoption of the CS approximation at the higher energies.

Quenching rate coefficients from initial rotational states, j_2=5, 10, 20, and 40, at temperatures ranging from 1 to 3000 K are shown in Figs. 2−9 for CO scattering with para- and ortho-H_2. Unfortunately, we are unaware of any experimental rate coefficient data for these initial states. Therefore, the current results are compared with the theoretical rate coefficients of Flower (2001), which were obtained over the limited temperature range, 5 to 400 K, with the V_{98} PES. Similar results with V_{04} were obtained by Wernli et al. (2006) for rotational levels of CO up to 5 and temperatures in the range 5−70 K. Wernli *et al.* also presented an analytic fit valid in the same temperature range. The rate coefficients calculated using their analytic relation are almost identical to the current results.

For the quenching of j_2=5 due to para-H_2 collisions, Fig. 2 shows that for temperatures

between ∼1 and 100 K, which is the van der Waals interaction-dominated regime, the rate coefficients exhibit an undulatory temperature dependence for $\Delta j_2 = -1$, -2, and -3 transitions due to the presence of resonances,[1] though the magnitude of the undulations decrease with increasing j_2. At temperatures above ∼100 K, the rate coefficients generally increase with increasing temperature. Comparison with the rate coefficients of Flower shows that at temperatures higher than ∼50 K, there is generally good agreement, except for $j_2' = 0$ and 2, where Flower's results get larger at temperatures above about 200 K. The results of Flower are smaller than the present rate coefficients for lower temperatures with the discrepancy increasing with decreasing temperature. Exceptions to this behavior are the transitions $j_2 = 5 \rightarrow j_2' = 2$ and 4, in which Flower's rate coefficients are generally larger than the present results. For quenching from initial levels j_2 =10 and 20 given in Figs. 3 and 4, respectively, the state-to-state rate coefficients have similar structure to that shown for $j_2 = 5$. The rate coefficients are dominated by small Δj_2. For $\Delta j_2 = -1$ transitions, a slight bump can be seen at temperatures between ∼1 and 100 K for $j_2 = 10$ and 20 as shown in Figs. 3 and 4. Figure 5 displays quenching rate coefficients for $j_2 = 40$. No previous results are available as the calculations of Flower (2001) stopped at $j_2 = 29$ for para-H_2 collisions.

For scattering by ortho-H_2, the trends noted for para-H_2 are also evident as displayed in Figs. 6-9. The quenching rate coefficients are of similar magnitude as those obtained for para-H_2 and show very similar structure. The highest level considered by Flower (2001) for ortho-H_2 collisions was $j_2 = 20$.

Comparing Figs. 2-9, some general trends can be noted. With few exceptions, the state-to-state rate coefficients appear to attain constant values as they decrease to 1 K.

---

[1]Additional typical examples of scattering resonances in cross section can be found in Yang et al. (2006a,b) along with rate coefficient comparisons for $j_2 < 4$.

However, this is deceptive as an orbiting resonance is typically present in the cross sections for collision energies between ∼0.01-1 cm^{-1} (see Fig. 1) computed on the V_{04} PES (Yang et al. 2006a). For temperatures less than shown, the rate coefficients typically decrease (increase) prior to the Wigner regime (Wigner 1948) for intermediate (high) j_2 before eventually attaining finite limiting values, typically below ∼1 mK.

Disregarding the effect of the resonances, one would expect two possible trends in the relative ordering of the rate coefficient values as a consequence of energy and angular momentum gaps. The exponential energy gap law (Steinfeld et al. 1991) predicts that the rate coefficients should decrease with increasing internal energy difference between the initial and final levels (i.e., with increasing $|\Delta j_2|$). However, CO is nearly homonuclear and rotational transitions in homonuclear molecules follow an even Δj_2 propensity rule (e.g., Shepler et al. 2007), though the effect may diminish for large values of $|\Delta j_2|$. Both effects appear to be important for CO-H_2. For example, $\Delta j_2 = -2$ is the dominant transition for quenching for temperatures greater than ∼1000-3000 K. It is also the dominant transition for temperatures less than ∼10 K, but only for $j_2 = 5$ and 10. For other temperatures, $\Delta j_2 = -1$ transitions are predominant, while for some cases $\Delta j_2 = -3$ is secondary, but with a rate coefficient larger than the $\Delta j_2 = -2$ transitions. However, for $\Delta j_2 < -3$, the exponential energy gap law appears to be fulfilled in nearly all considered cases.

5. ASTROPHYSICAL IMPLICATIONS

As discussed in the introduction, carbon monoxide plays an important role in a variety of astrophysical and atmospheric environments and has been detected in countless sources under a variety of excitation conditions. We discuss a few of these below focusing primarily on observed and predicted transitions from intermediate- and high-j_2 in the FIR.

Rotational emission lines of CO have been observed in high-redshift (z) objects including the quasar SDSS J1148+5251 at $z = 6.42$ using the Very Large Array. Narayanan et al. (2008) modeled the emission from CO($v = 0, j_2$) with $j_2 = 1 - 10$ with a non-LTE radiative transfer code and considered excitation due to H_2 with rate coefficients taken from the LAMDA database. They found that the CO spectral energy distribution (SED) peaks at $j_2 = 8$ at the beginning of the quasar phase, $z \sim 7 - 8$. Observations and modeling of the CO emission can serve to probe the hierarchical buildup of the host galaxy and the quasar phase and can be used to estimate the halo mass and quasar host morphology.

Spaans & Meijerink (2008) proposed that CO emission from j_2 as high as 30 could be observed from high-z massive accreting black holes using the Atacama Large Millimeter/submillimeter Array (ALMA). Such observations could provide a diagnostic of the radiation source: PDR or x-ray dominated region (XDR), for example. However, as the densities of such objects are typically 10^5 cm^{-3}, collisions with the dominant species, H_2, will determine the CO rotational populations. In Fig. 10, the critical densities for CO due to para-H_2 collisions are plotted (neglecting optical depth effects) where the critical density of rotational level j_2 is defined as

$$n_{\rm cr}(j_2) = \frac{\sum_{j_2'<j_2} A_{j_2 \rightarrow j_2'}}{\sum_{j_2' \neq j_2} k_{j_2 \rightarrow j_2'}(T)} \tag{2}$$

(e.g., Osterbrock & Ferland 2006) and $A_{j_2 \rightarrow j_2'}$ are the spontaneous transition probabilities for dipole transitions. Rotational levels $j_2 \gtrsim 10$ are seen to be clearly out of thermal equilibrium for a gas density of 10^5 cm^{-3} requiring a non-LTE analysis. As the LAMDA database incorporates the CO-H_2 rate coefficients of Wernli et al. (2006) and Flower (2001) with extrapolations for para- and ortho-H_2 collisions above $j_2 = 29$ and 20, respectively, the predicted CO line intensities of Spaans & Meijerink (2008) for emission from levels larger than $j_2 = 20$ would likely be improved if the current rate coefficients are adopted.

Interestingly, their predicted CO SEDs peak at $j_2 = 10$ and $j_2 = 25$ for PDR and XDR environments, respectively.

The $j_2 = 6 \rightarrow 5$ and $j_2 = 7 \rightarrow 6$ lines have been observed in the starburst galaxy NGC 253 (Hailey-Dunsheath et al. 2008; Bradford et al. 2003). Using a non-LTE analysis, Bradford et al. (2003) concluded that the cooling in the CO lines is so large that it must be balanced by a cosmic ray heating rate ∼800 times greater than that in the Milky Way. Previously, Krolik & Lepp (1989) suggested that highly-excited j_2 lines (e.g., $j_2 = 16 - 58$) could be detectable from Seyfert galaxies giving diagnostics of the internal pressure of the dust-obscured torus.

The *Infrared Space Observatory* studied a large variety of pre-main sequence objects (i.e., protostars) and detected numerous FIR CO rotational lines. For example, emission lines from $j_2 = 14 - 26$ were observed in the Class 0 object L1448-mm (Nisini et al. 1999), $j_2 = 14 - 31$ in the Class I object IC 1396N, $j_2 = 14 - 16$ in the Class I object W28 A2, $j_2 = 14 - 20$ in the Class II object R CrA (Saraceno et al. 1999), and $j_2 = 14 - 25$ in T Tauri (Spinoglio et al. 1999). Non-LTE analyses of these pre-main sequence objects suggested multiple components with various excitation conditions. Future studies of these protostars, the infrared sources discussed above, and future FIR and submillimeter observations with *Herschel* and ALMA can benefit from the CO-H_2 quenching rate coefficients presented here.

6. CONCLUSIONS

Rotational quenching of CO due to para- and ortho-H_2 collisions has been studied using an explicit quantum-mechanical close-coupling approach and the coupled-states approximation on the potential surface, V_{04}, of Jankowski & Szalewicz (2005). State-to-state quenching rate coefficients for initial rotational levels j_2 =1, 2, $\cdots$, 40 of CO are

obtained over a wide temperature range and available in tables formatted for astrophysical applications. Resonances result in undulations in the temperature dependence of the rate coefficients with the amplitudes of the undulations typically decreasing with j_2. For temperatures less than ∼50 K, the current state-to-state rotational quenching rate coefficients obtained with V_{04} are found to depart from the results of Flower (2001) obtained with the earlier V_{98} PES. The discrepanices are likely related to the differences in the well depth and anisotropy of the two potentials.

BHY and PCS acknowledge support from NASA grant NNX07AP12G. NB acknowledges support from NSF through grant PHY-0855470. RCF acknowledges support from NSF through grant PHY-0854838. We thank Dr. Piotr Jankowski for providing his CO-H_2 potential subroutine and Prof. Gary Ferland and Dr. Donghui Quan for discussions on astrophysical applications. Part of calculations were performed on EITS/RCC pcluster at the University of Georgia.

REFERENCES

Alexander, M. H., & Manolopoulos, D. E. 1987, J. Chem. Phys., 86, 2044

Andresen, P., Joswig, H., Pauly, H., & Schinke, R. 1982, J. Chem. Phys., 77, 2204

Antonova, S., Tsakotellis, A. P., Lin, A., & McBane, G. C. 2000, J. Chem. Phys., 112, 554

Bacic, Z., Schinke, R., & Diercksen, G. H. F. 1985, J. Chem. Phys., 82, 236

Bacic, Z., Schinke, R., & Diercksen, G. H. F. 1985, J. Chem. Phys., 82, 245

Baker, D. J., & Flower, D. R. 1984, J. Phys. B, 17, 119

Bouanich, J. P., & Brodbeck, C. 1973, J. Quant. Spectrosc. Radiat. Trans., 13, 1

Bradford, C. M. et al. 2003, ApJ, 586, 891

Brechignac, P., Picard-Bersellini, A., Charneau, R., & Launay, J. M. 1980, Chem. Phys., 53, 165

Butz, H. P., Feltgen, R., Pauly, H., & Vehmeyer, H. 1971, Z. Phys., 247, 70

Danby, G., Furlong, J., Lodge, D., Miller, S., & Patel, A. 1993, J. Phys. B, 26, 4127

Drascher, T. et al. 1998, J. Mol. Spectrosc., 192, 268

Flower, D. R., Launay, J. M., Kochanski, E., & Prissette, J. 1979, Chem. Phys., 37, 355

Flower, D. R. & Launay, J. M. 1985, MNRAS, 214, 271

Flower, D. R. 2001, J. Phys. B, 34, 2731

Gottfried, J., & McBane, G. C. 2000, J. Chem. Phys., 112, 4417

Green, S. 1975, J. Chem. Phys., 62, 2271

Green, S., & Thaddeus, P. 1976, ApJ, 205, 766

Heiley-Dunsheath, S. et al. 2008, ApJ, 689, L109

Heil, T. G., Green, S., & Kouri, D. J. 1978, J. Chem. Phys., 68, 2562

Herbst, E. 2001, Chem. Soc. Rev., 30, 168

Huber, K. P., Herzberg, G., 1979, Molecular Spectra and Molecular Structure. IV. Constants of Diatomic Molecules, Van Nostrand Reinhold Co.

Hutson, J. M., & Green, S. 1994, MOLSCAT computer code, version 14, Collaborative Computational Project No. 6 of the Engineering and Physical Sciences Research Council (UK)

Jankowski, P., & Szalewicz, K. 1998, J. Chem. Phys., 108, 3554

Jankowski, P., & Szalewicz, K. 2005, J. Chem. Phys., 123, 104301

Jones, H. R. A., Pavlenko, Y. V., Viti, S., Barber, R. J. Yakovina, L. A., Pinfield, D., & Tennyson, J. 2005, MNRAS, 358, 105

Krolik, J. H. & Lepp, S. 1989, ApJ, 347, 179

Kudian, A., Welsh, H. L., & Watanabe, A. 1967, J. Chem. Phys., 47, 1553

Kuppermann, A., Gordon, R. J., & Coggiola, M. J. 1973, Faraday Discuss. Chem. Soc., 55, 145

Le Petit, F., Nehmé, C., Le Bourlot, J., & Roueff, E., 2006, ApJS, 164, 506

Liszt, H. S. 2006, A&A, 458, 507

Liszt, H. S. 2007, A&A, 476, 291

Lovas, F. J., Johnson, D. R., & Snyder, L. E., 1979, ApJS, 41, 451

McKellar, A. R. W. 1990, J. Chem. Phys., 93, 18

McKellar, A. R. W. 1991, Chem. Phys. Lett., 186, 58

McKellar, A. R. W. 1998, J. Chem. Phys., 108, 1811

Mengel, M., DeLucia, F. C., & Herbst, E. 2001, Can. J. Phys., 79, 589

Narayanan, D. et al. 2008, ApJ Supplement Series, 174, 13

Nerf, R. B., Jr., & Sonnenberg, M. A. 1975, J. Mol. Spectrosc., 58, 474

Nisini, B., et al. 1999, A & A, 350, 529

Osterbrock, D. E. & Ferland, G. J. 2006, Astrophysics of Gaseous Nebulae and Active Galactic Nuclei, 2nd ed. (University Science, Sausalito)

Parish, C. A., Augspurger, J. D., & Dykstra, C. E. 1992, J. Phys. Chem., 96, 2069

Pavlenko, Y. V., & Jones, H. R. A. 2002, A&A, 396, 967

Picard-Bersellini, A., Charneau, R., & Brechignac, P. 1983, J. Chem. Phys., 78, 5900

Poulsen, L. L. 1982, Chem. Phys., 68, 29

Prisette, J., Kochanski, E., & Flower, D. R. 1978, Chem. Phys., 27, 373

Reid, J. P., Simpson, C. J. S. M., & Quiney, H. M. 1997, J. Chem. Phys., 106, 4931

Röllig, M. *et al.* 2007, A&A, 467, 187

Salazar, M. C., de Castro, A., Paz, J. L., Diercksen, G. H. F., & Hernandez, A. J. 1995, Int. J. Quantum Chem., 55, 251

Salyk, C., et al. 2008, ApJ, 676, L49

Saraceno, P., et al. 1998, Proceedings of the Conference *The Universe as seen by ISO*, p. 575

Schinke, R., Meyer, H., Buck, U., & Diercksen, G. H. F. 1984, J. Chem. Phys., 80, 5518

Schöier, F. L., van der Tak, F. F. S., van Dishoeck, E. F., & Black, J. H. 2005, A&A, 432, 369

Schramm, B., Elias, E., Kern, L., Natour, G., Schmitt, A., & Weber, C. 1991, Ber. Bunsenges. Phys. Chem., 95, 615

Schweitzer, A., Hauschildt, P. H., & Baron, E. 2000, ApJ, 541, 1004

Shaw, G., Ferland, G. J., Abel, N. P., Stancil, P. C., & van Hoof, P. A. M. 2005, ApJ, 624, 794

Shepler, B. C., Yang, B. H., Dhilip Kumar, T. J., Stancil, P. C., Bowman, J. M., Balakrishnan, N., Zhang, P., Bodo, E., & Dalgarno, A. 2007, A&A, 475, L15

Snow, T. P., & McCall, B. J. 2006, Annu. Rev. Astro. Astrophys., 44, 367

Sonnentrucker, P., Welty, D. E., Thorburn, J. A., & York, D. G. 2007, ApJ Suppl., 168, 58

Spaans, M. & Meijerink, R. 2008, ApJ, 678, L5

Spinoglio, L., et al. 1998, Proceedings of the Conference *The Universe as seen by ISO*, p. 517

Steinfeld, J. I., Ruttenberg, P., Millot, G., Fanjoux, G., & Lavorel, B. 1991, J. Phys. Chem., 95, 9638

Swain, M. R., et al. 2009, ApJ, 690, L114

van Dishoeck, E. F., & Black, J. H. 1988, ApJ, 334, 771

van Hemert, M. C. 1983, J. Chem. Phys., 78, 2345

Warin, S., Benayoun, J. J., & Viala, Y. P. 1996, A&A, 308, 535

Wernli, M., Valiron, P., Faure, A., Wiesenfeld, L., Jankowski, P., & Szalewicz, K. 2006, A&A, 446, 367

Wigner, E. P. 1948, Phys. Rev., 73, 1002

Yang, B. H., Stancil, P. C., Balakrishnan, N., & Forrey, R. C. 2006, J. Chem. Phys., 124, 104304; erratum 125, 079904

Yang, B. H., Perera, H., Balakrishnan, N., & Forrey, R. C., & Stancil, P. C. 2006, J. Phys. B, 39, S1229

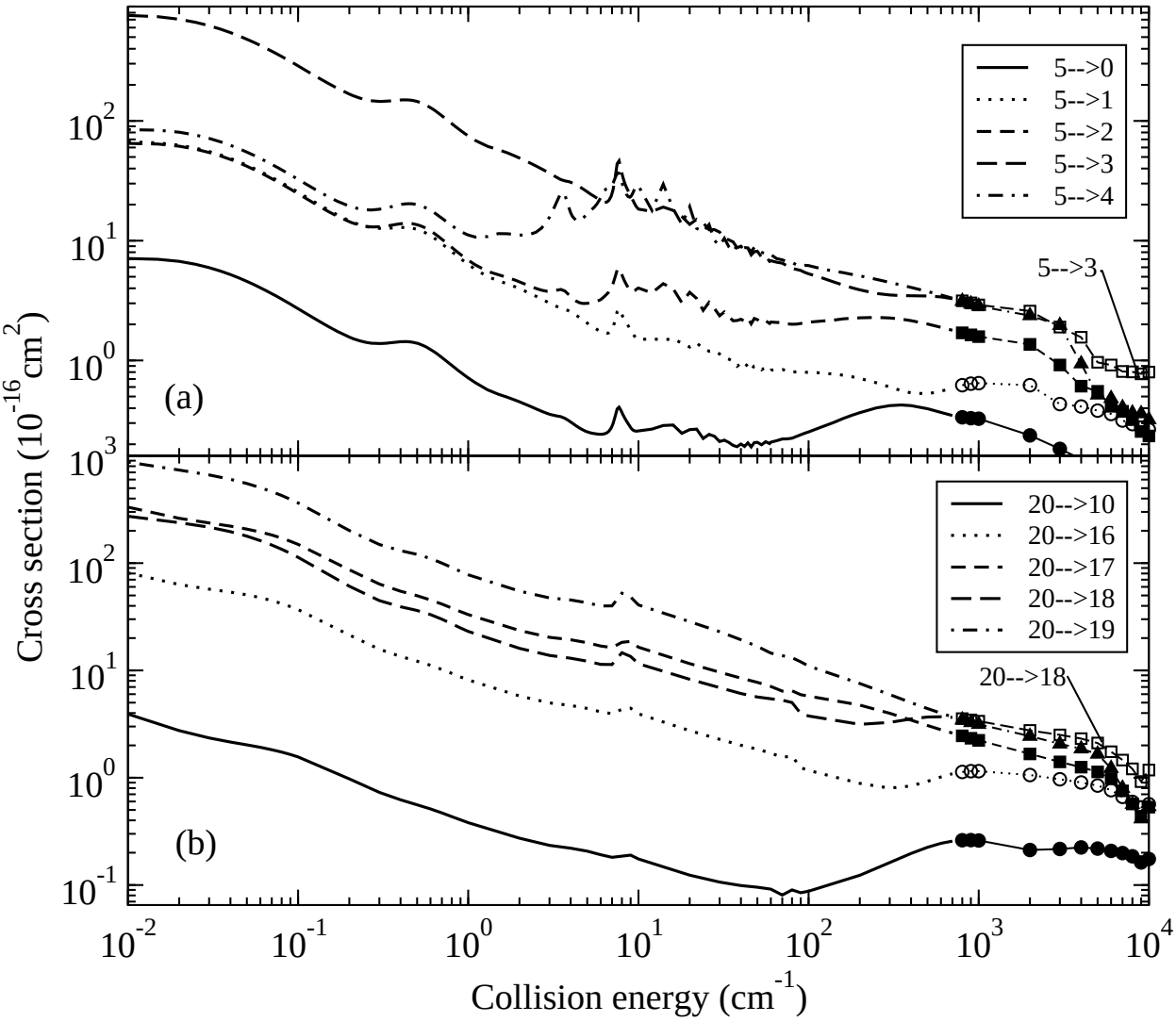

Fig. 1.— Cross sections for the quenching of CO(j_2) due to para-H_2 collisions as a function of collision energy obtained with the close-coupling method (lines) and coupled-states approximation (symbols). (a) $j_2 = 5$, (b) $j_2 = 20$.

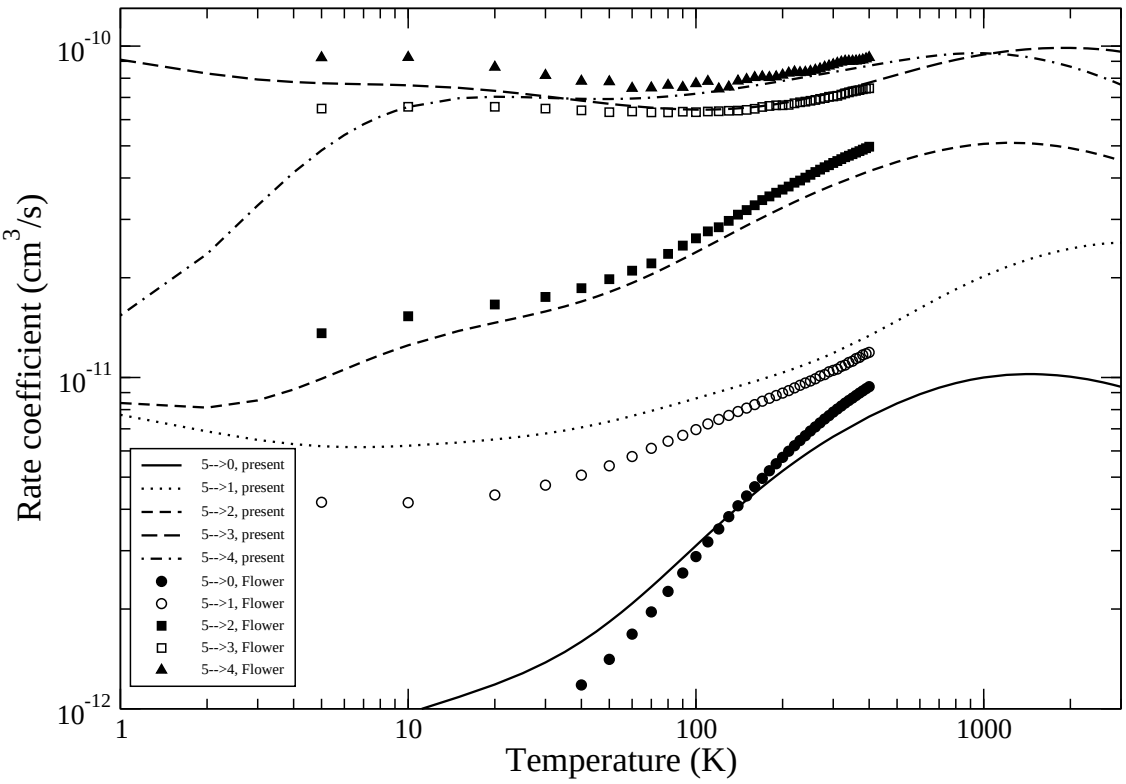

Fig. 2.— Rate coefficients for the quenching of CO(j_2=5) by collisions with para-H_2 as functions of temperature. Lines indicate present calculations on potential V_{04}, symbols denote the results of Flower (2001) on potential V_{98}. Solid line and solid circles: $j_2 = 5 \rightarrow j_2' = 0$, dotted line and open circles: $j_2 = 5 \rightarrow j_2' = 1$, dashed line and solid squares: $j_2 = 5 \rightarrow j_2' = 2$, dot-dash line and solid squares: $j_2 = 5 \rightarrow j_2' = 3$, double-dot-dash line and solid triangles: $j_2 = 5 \rightarrow j_2' = 4$.

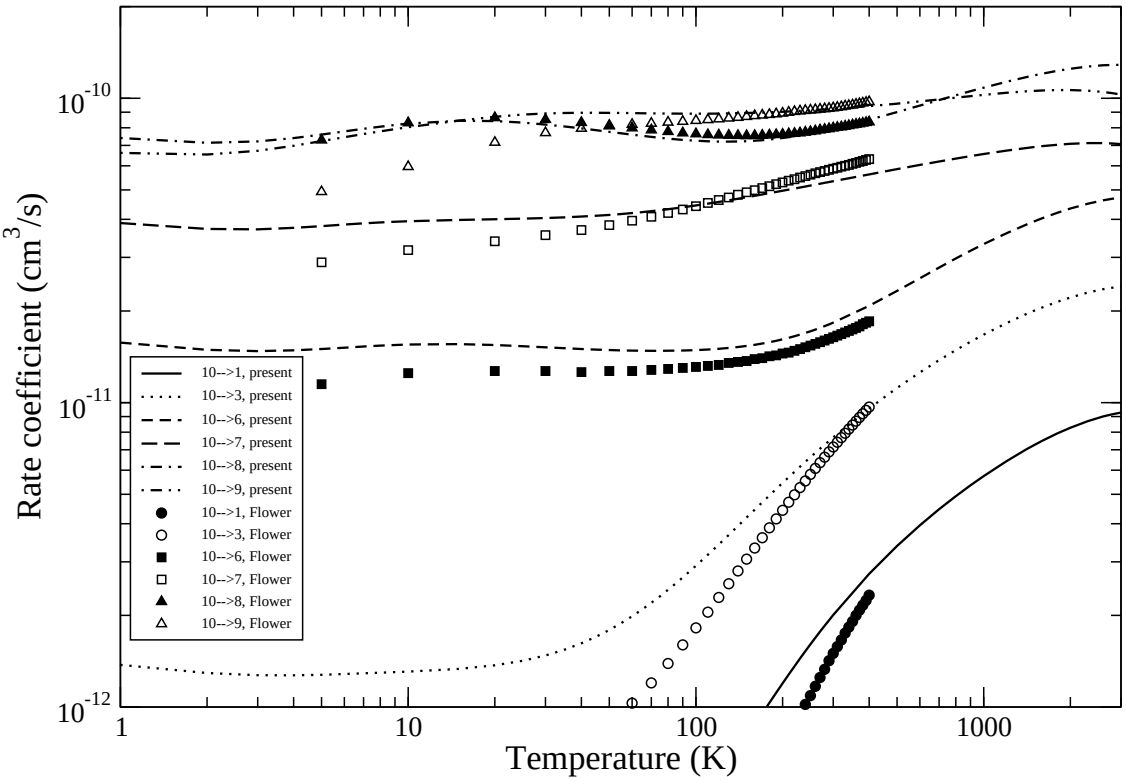

Fig. 3.— Same as Fig. 2, except for $j_2 = 10$ and j_2' as indicated.

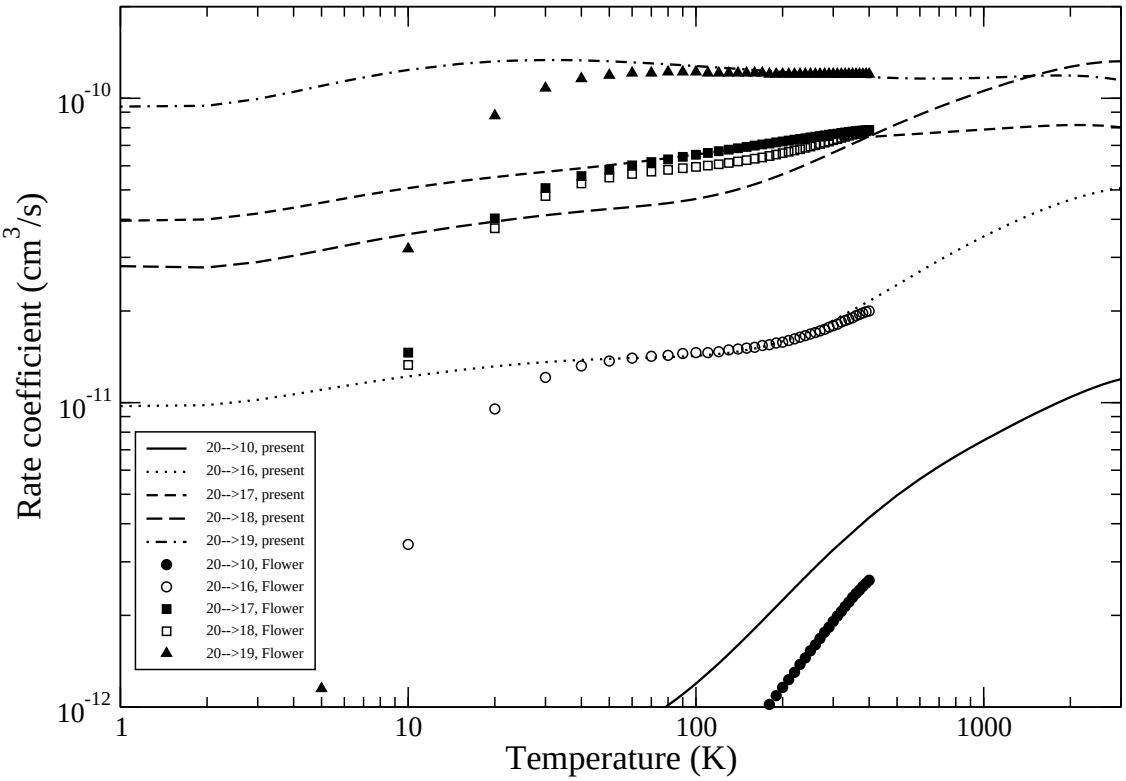

Fig. 4.— Same as Fig. 2, except for $j_2 = 20$ and j_2' as indicated.

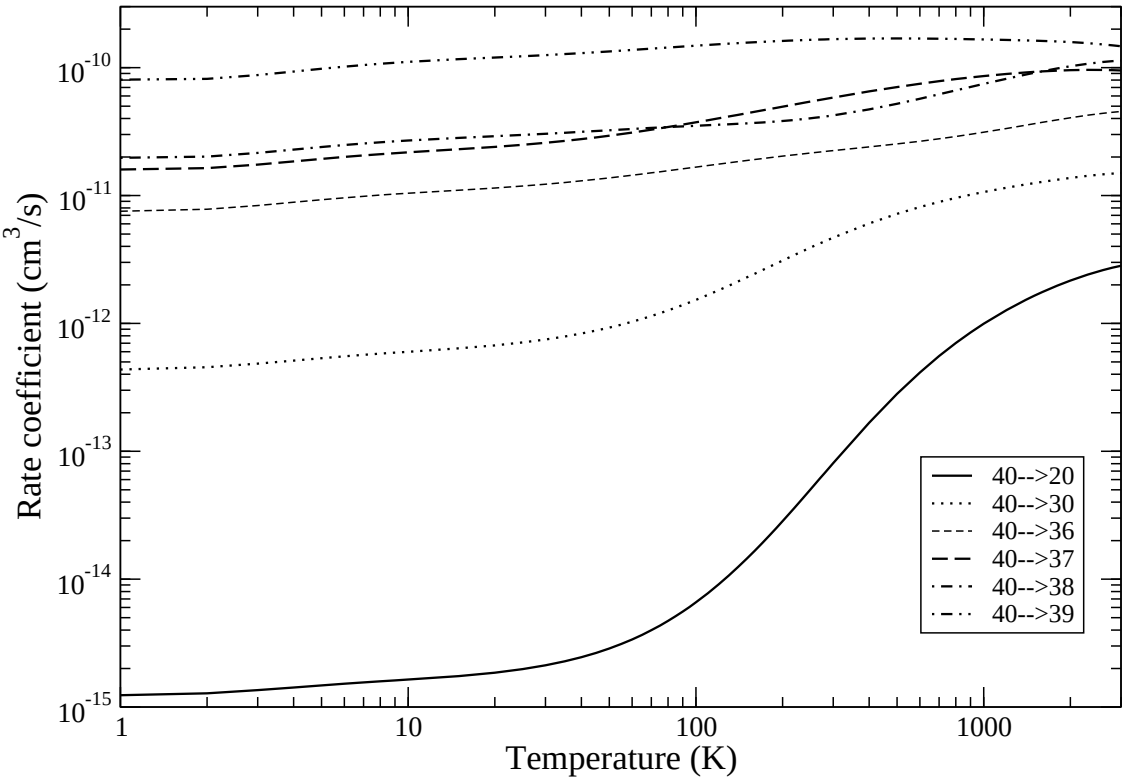

Fig. 5.— Same as Fig. 2, except for $j_2 = 40$ and j_2' as indicated.

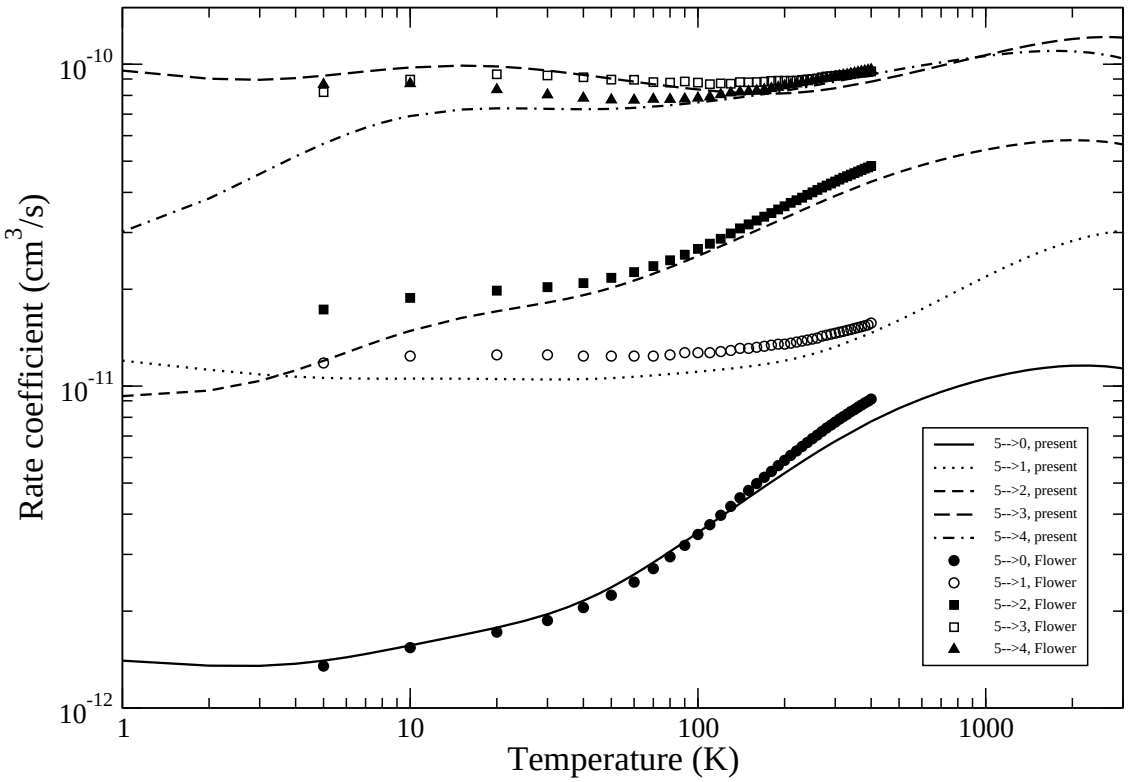

Fig. 6.— Same as Fig. 2, except for ortho-H_2.

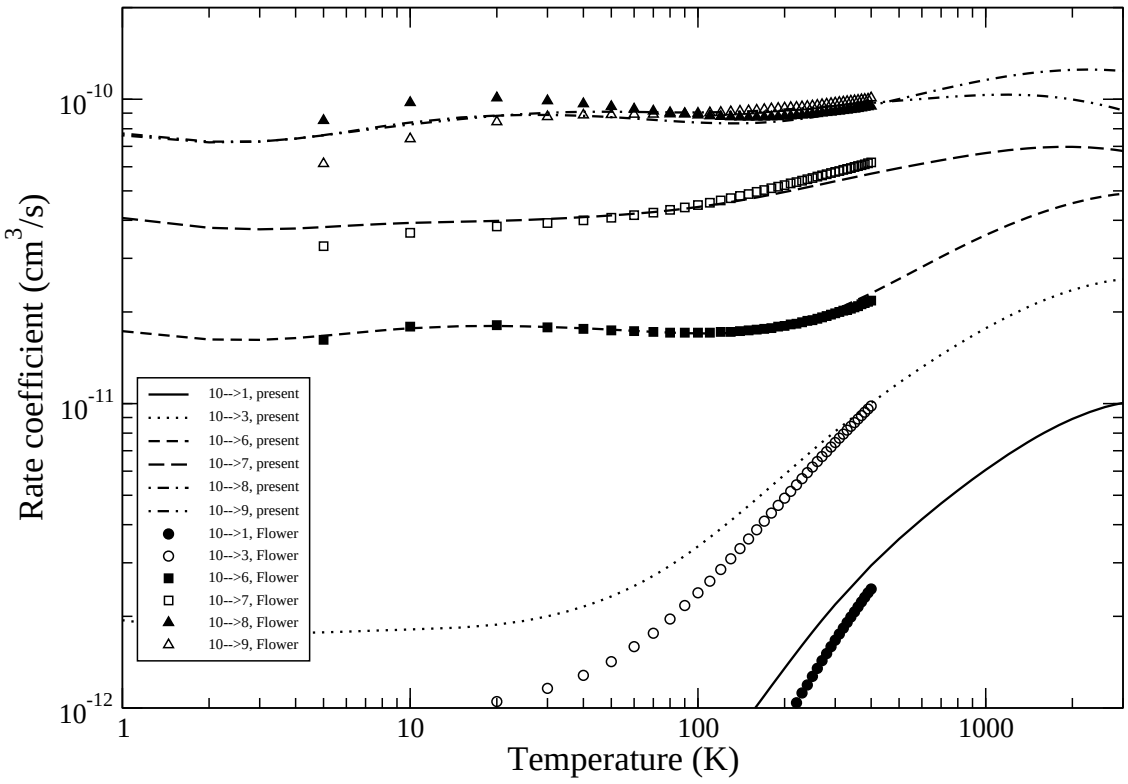

Fig. 7.— Same as Fig. 3, except for ortho-H_2.

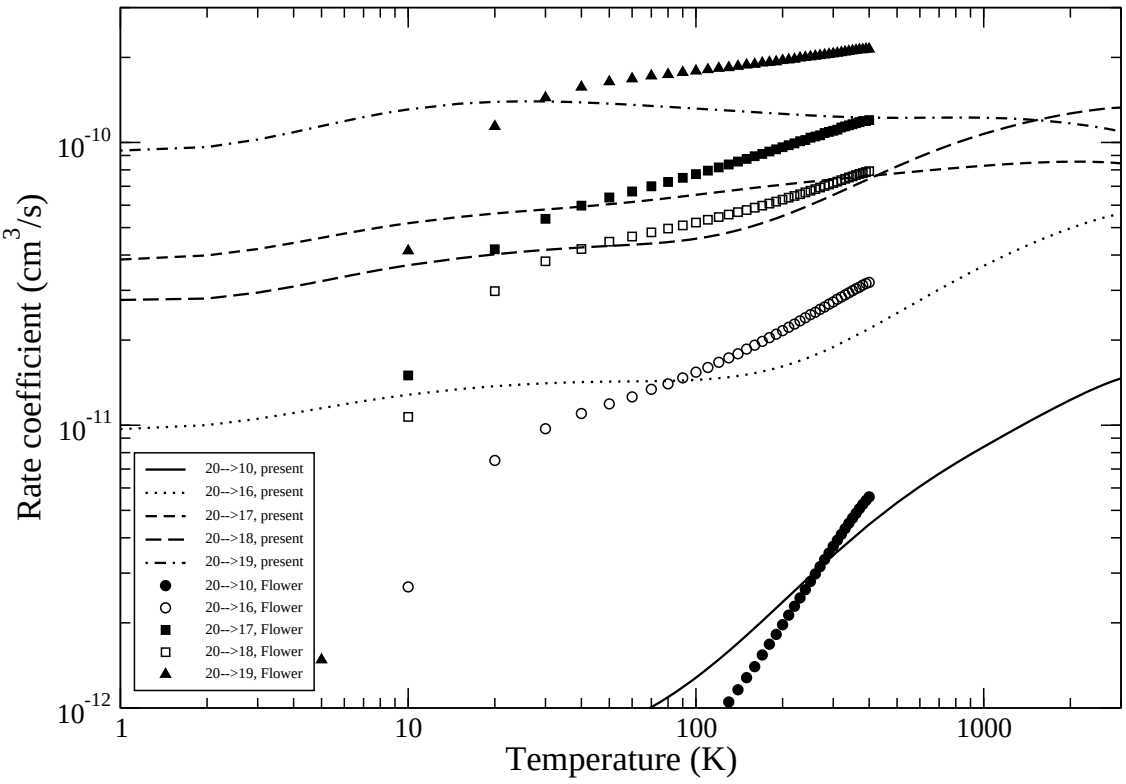

Fig. 8.— Same as Fig. 4, except for ortho-H_2.

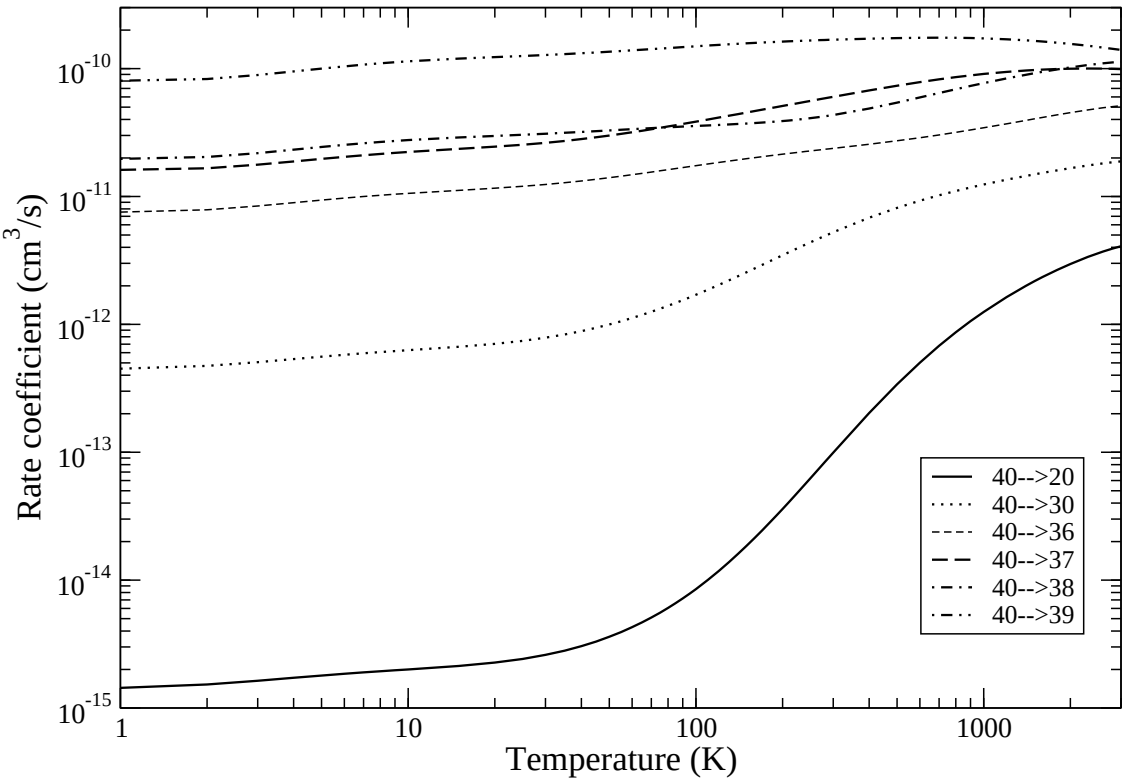

Fig. 9.— Same as Fig. 5, except for ortho-H_2.

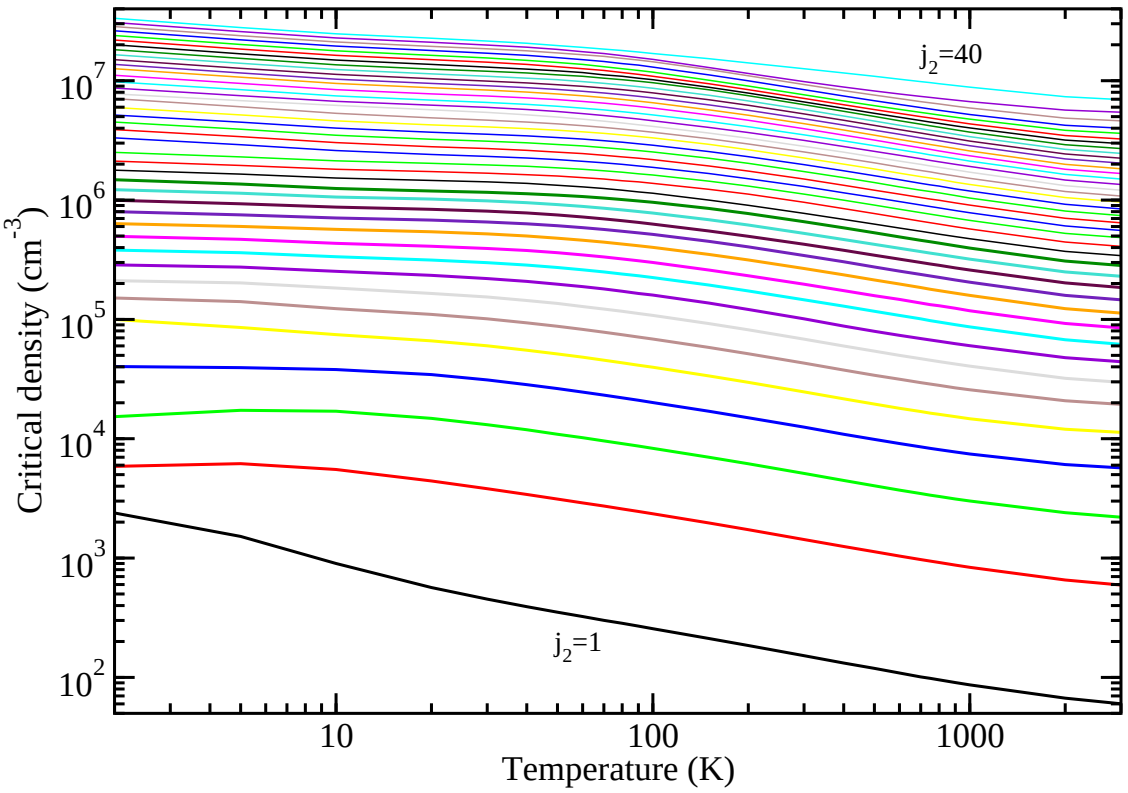

Fig. 10.— Critical densities for CO($v = 0, j_2$) due to para-H_2 collisions as a function of gas temperature T.